Spin Transition during H 2 O 2 Formation in the Oxidative Half-Reaction of Copper Amine Oxidases

ARTICLE *in* THE JOURNAL OF PHYSICAL CHEMISTRY B · SEPTEMBER 2004

Impact Factor: 3.3 · DOI: 10.1021/jp0478312

Spin Transition during H_2O_2 Formation in the Oxidative Half-Reaction of Copper Amine Oxidases

Rajeev Prabhakar* and Per E. M. Siegbahn

Department of Physics, Stockholm Centre for Physics, Astronomy and Biotechnology, Stockholm University, S-106 91 Stockholm, Sweden

Boris F. Minaev and Hans Ågren

Laboratory of Theoretical Chemistry, Stockholm Centre for Physics, Astronomy and Biotechnology, The Royal Institute of Technology, SE-10044 Stockholm, Sweden

Received: May 19, 2004

Dioxygen reduction in the oxidative half-reaction of copper amine oxidases (CAOs) has been studied quantum chemically using the hybrid density functional theory (B3LYP). The reductive activation of dioxygen is a spin-forbidden process for which substantial kinetic O-18 (but no deuterium) isotope effects have been found experimentally. The proposed mechanism was divided into three steps, and the last step was studied for two different potential energy surfaces: the quartet and the doublet surfaces. It is suggested that dioxygen reduction occurs through a spin transition that is induced by the exchange interaction between the unpaired spins of the Cu(II) ion and the O_2^- anion. The step involving this spin transition is suggested to be rate-limiting, which gives a rationalization for the puzzling experimental results when copper is substituted for other metals. The spin transition is triggered by the calculated vibronic perturbation of 5.4 (kcal/mol) $Å^{-1}$, which leads to a very fast rate of 8×10^{10} s^{-1} for the spin transition. However, since the spin transition occurs at a calculated energy that is 18−20 kcal/mol higher than that of the reactant, this step could still be rate-limiting. The difference in the O−O bond distance between the resting state (free dioxygen) and the point of the spin transition provides an explanation for the oxygen isotope effect.

I. Introduction

Molecular oxygen is required by organisms in oxidative metabolic processes, in respiration, and in degradation of food to water, carbon dioxide, and dinitrogen.[1,2] Oxygen is a stable biradical with two unpaired electrons generating the triplet $X^3\Sigma_g^-$ ground state of the O_2 molecule. Triplet dioxygen possesses a paramagnetic character and a very sluggish kinetic reactivity. Aerobic life is kinetically stable with respect to oxidation by O_2 in the air. The origin of this stability is determined by the spin prohibition for the triplet oxygen reactions.[3] The direct interaction of O_2 with C=C groups, for example, leads to the formation of biradicals, where spin−orbit coupling is suppressed by orbital symmetry,[3] and production of radicals therefore is the only way to overcome the spin prohibition. This is a highly endergonic ignition process.[4] Thus, combustion requires a high-temperature initiation step for starting the radical-chain process, and it releases energy without strong regulation. In contrast, the oxygenase enzymes control the specific reaction pathways of triplet dioxygen by subtle spin-selective processes that store and smoothly release energy. Enzymes activate triplet dioxygen in a stepwise manner via electron and proton transfers and the formation of biradical intermediates:[2]

$$MH + O_2 \rightarrow MH^+ + O_2^- \quad (1)$$

$$O_2^- + H^+ \rightarrow HO_2 \quad (2)$$

$$HO_2 + MH^+ \rightarrow H_2O_2 + M^+ \quad (3)$$

Here, MH is a closed-shell cofactor in the enzyme, such as TPQ in copper amine oxidases (CAOs)[5] or $FADH_2$ in glucose oxidase (GO).[5,6] If the closed-shell cofactor MH is involved as an electron donor for the reduction of dioxygen, the production of closed-shell species is spin-forbidden. After the electron-transfer step (eq 1), the $O_2^-\cdots MH^+$ radical pair is in a triplet state. The proton transfer (eq 2) does not change the spin multiplicity of the electronic system. However, at the stage of hydrogen peroxide production (eq 3), the system has a singlet ground state. The chemical transformation, which starts in the triplet spin state (eq 1) and accomplishes hydrogen peroxide production (eq 3), finishes at the singlet-state potential energy surface (PES). Thus, enzymes such as CAOs have to find a way to produce a spin transition in order to complete hydrogen peroxide production. CAOs and many other metal-containing enzymes can utilize the exchange interaction between the unpaired spin of the metal ion and the O_2^- anion for the intersystem crossing (ISC) in the $MH^+\cdots O_2^-$ radical pair. Even if there is no chemical bonding between the metal ion and oxygen (i.e., only electrostatic stabilization), the spin exchange can still occur and can be induced by intermolecular vibrations.[7] Spin exchange between colliding radicals is a well-known dynamic process in solvents; it is detected by the line shape of the EPR signal and is induced by exchange interactions.[8,9] The spin exchange between a paramagnetic metal ion and oxygen is relatively strong if they are in the proximity of each other during the vibrational movement of the highest amplitude at the enzyme active site. In contrast, the exchange interaction between the spin on a metal and an organic MH^+ cation is completely negligible. This difference in exchange interactions leads to a spin transition in the $MH^+\cdots O_2^-$ radical pair, but the total spin of the

* Corresponding author.

10.1021/jp0478312 CCC: $27.50
Published on Web 08/10/2004

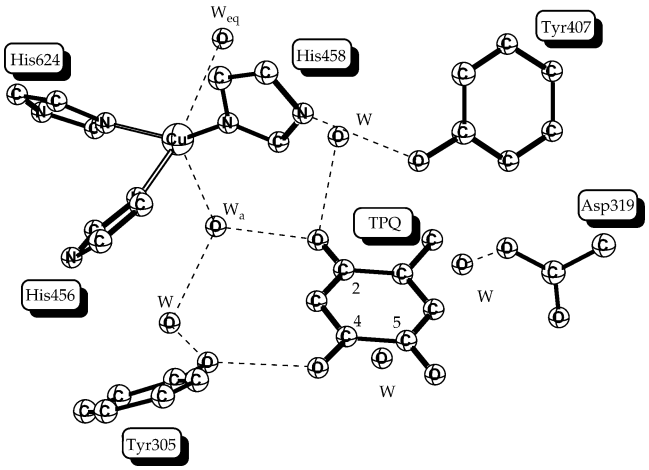

Figure 1. X-ray structure of the active-site region of HPAO.

$MH^+\cdots O_2^-\cdots$Cu(II) system remains unchanged. Thus, ISC mechanisms are likely to be induced by the vibronic interactions and spin−orbit coupling (SOC) in the O_2^- anion in enzymes, such as glucose oxidase (GO),[6] where there is no metal present. Vibronic-induced exchange interactions with a metal ion are similar in the way that the spin−flip occurs in the superoxide anion.

The CAO enzymes are homodimeric with 70−95 kDa subunits. They catalyze the two-electron oxidative deamination of primary amines by dioxygen to corresponding aldehydes, ammonia, and hydrogen peroxide.[10] The crystal structures from *Escherichia coli* (ECAO),[11] pea seedling (PSAO),[12] yeast *Hansenula polymorpha* (HPAO),[13] and *Arthrobacter globiformis* (AGAO)[14] have been solved. Recently Zn- and Ni-substituted structures from AGAO have been crystallized.[15] All CAOs contain a peptide-bound quinone cofactor, 2,4,5-trihydroxyphenylalaninequinone, termed topa quinone (TPQ). CAOs are known to be dual-function enzymes, catalyzing both the formation of TPQ through the oxygenation of tyrosine and the oxidation of amines within a single active site. The catalytic mechanism for the biogenesis and turnover of cofactor TPQ has been reviewed several times.[16−20] Catalysis is suggested to proceed through a ping-pong-type mechanism in two half-reactions known as the reductive and oxidative half-reactions.

$$E_{ox} + RCH_2NH_2 \rightarrow E_{red} + RCHO \quad (4)$$

$$E_{red} + O_2 + H_2O \rightarrow E_{ox} + H_2O_2 + NH_3 \quad (5)$$

In the reductive half-reaction, TPQ is reduced by the substrate amine to an aminophenol species, which is reoxidized back to TPQ by the molecular oxygen in the oxidative half-reaction. Both the reductive and oxidative half-reactions have been studied extensively by experimental and theoretical methods.[21−27] In the crystal structure of HPAO (solved to 2.4 Å resolution),[13] shown in Figure 1, the active-site copper atom is pentacoordinated to the imidazole side chains of His456, His458, and His624, and to two water molecules, one axial and one equatorial in a distorted square-pyramidal geometry. The active-site base Tyr305 and another water molecule participate in a hydrogen-bonded network, which connects the O-2 and O-4 sites of TPQ. During the catalytic cycle, the copper-metal center, positioned very close to the O_2 binding site,[13,28] is suggested to be in the paramagnetic Cu(II) oxidation state.[29]

Of the experimentally suggested mechanisms[24,29] for dioxygen reduction, the most accepted one[29] is shown in Figure 2. The mechanism is divided into four steps. In the first step, dioxygen

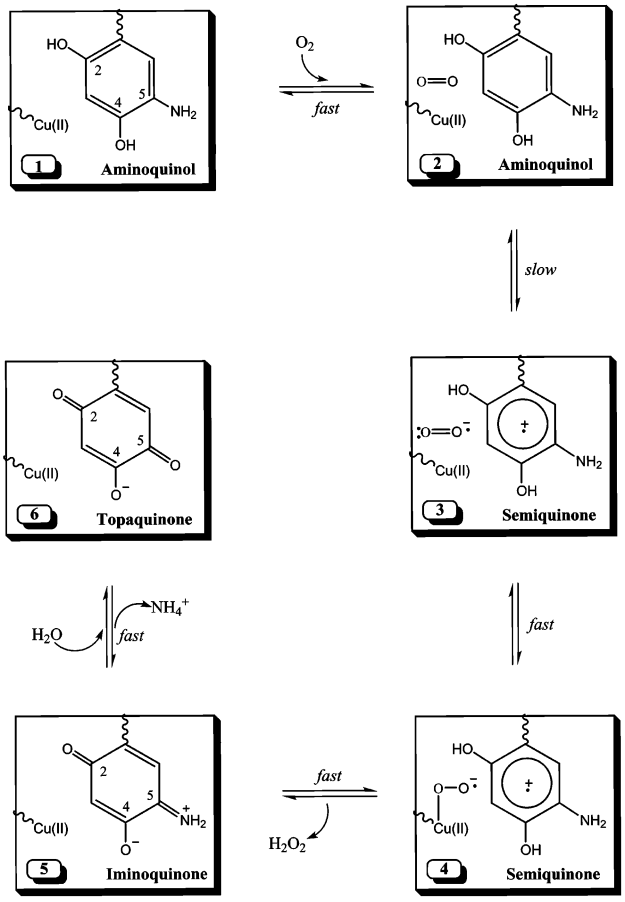

Figure 2. Experimentally suggested mechanism for the dioxygen reduction in CAO.

binds at a specific non-metal site where it can accept an electron from the TPQ cofactor. The X-ray crystal structures of CAOs indicate the existence of a highly hydrated dimer interface between the two subunits.[11,13,14] Dioxygen has been suggested to be dissolved in this hydrated interface before entering into the active site through a discrete channel which leads toward the non-metal binding site. The dioxygen binding site has been located in HPAO as a patch consisting of three hydrophobic amino acids, Tyr407, Leu425, and Met634. This cavity lies in the vicinity of the O-2 position of the cofactor and is equatorial to copper.[29] When systematic changes were made in the side chain of the Met634 residue in HPAO, a strong correlation was found between the size of this residue and the magnitude of k_{cat}/K_M (O_2) but with relatively small effects on k_{cat}.[20] Since k_{cat} is limited by the TPQ oxidation, the size of the active-site Met634 residue has been suggested to influence the access of dioxygen to the hydrophobic cavity.

In the second step of the suggested mechanism, dioxygen reduction is triggered by the first electron transfer from TPQ_{red} to dioxygen which leads to the formation of the superoxide anion. A measured O-18 kinetic isotope effect of 1.01 kcal/mol has been used to suggest that the first electron transfer from TPQ_{red} to dioxygen is rate-limiting for BSAO (bovine serum amine oxidase)[29] and HPAO.[30] The size of the isotope effect is somewhat smaller than the calculated value of 1.03 kcal/mol for the conversion of O_2 to a superoxide anion.[32] Small conformational changes in the copper−metal complex were therefore suggested to significantly influence the size of the O-18 kinetic isotope effect.[20] Solvent viscosogen experiments confirmed that dioxygen binding is not part of the rate-limiting step, that is, dioxygen must prebind to the enzyme prior to the rate-

determining electron-transfer step.[1,29] It has furthermore been observed that the electron transfer is followed by the displacement of a metal-bound water molecule in the wild-type (WT) and Co-substituted HPAO.[30] The conclusion that the first electron transfer is rate-limiting was supported by the estimated negative redox potential of <0.16 V for the formation of the superoxide anion in relation to the estimated potential for TPQ_{sq}/TPQ_{red} of >0.1 V at pH 7.0.[29] These redox potentials in solution suggest that this electron transfer is thermodynamically unfavorable by >6 kcal/mol. The rate of electron tunneling could also be affected by the unfavorable driving force and the Franck−Condon barrier. In model compounds, studied at pH 7.1,[31] the measured rate (k_{cat}) of 18.6 M^{-1} s^{-1} for TPQ_{red} oxidation by dioxygen was found to be 10^4-fold slower than in the enzyme,[32] indicating a direct interaction between dioxygen and the metal. The substitution of Cu^{2+} with the diamagnetic Ni^{2+} and Zn^{2+} ions in HPAO resulted in substantially reduced catalytic activities. On the other hand, the Cu^{2+} substitution with paramagnetic Co^{2+} did not alter the k_{cat}[32] value but decreased k_{cat}/K_M for O_2 by 250-fold.[30] Wild-type and Co(II)-substituted HPAOs have almost identical properties, for example, (1) no dependence on solvent viscosogen, (2) small solvent isotope effects, and (3) very similar O-18 isotope effects.[30] They are therefore suggested to follow very similar mechanisms but with one difference; in WT-HPAO, one of the copper-bound water molecules loses a proton, which is not the case for cobalt. Although it is not known with certainty, this difference in charge is expected to decrease the affinity of O_2 for binding at the hydrophobic site, thereby decreasing k_{cat}/K_M for O_2.[30] However, in AGAO, the substitution of Cu^{2+} with Ni^{2+} and Co^{2+} did not change the K_M but reduced the k_{cat} by 100-fold.[15] At this point, the reason for the difference observed between eukaryotic HPAO and bacterial AGAO is not clear. In the third step of the suggested mechanism, the superoxide anion formed in the previous step is suggested to interact with the copper-metal ion.[32] Two different mechanisms, "copper-on" and "copper-off" have been suggested.[24,29] According to the copper-on mechanism, the superoxide anion moves and forms a bond to copper,[29] while in the copper-off mechanism, the superoxide anion does not bind to copper.[29] The former mechanism is supported by the crystal structure from ECAO where a peroxy species is directly bonded to the Cu ion.[28] The inability of Zn(II)- and Ni(II)-substituted enzymes to support catalysis suggests the involvement of something more than a mere electrostatic interaction between the Cu(II) ion and the superoxide anion, possibly involving the charge transfer.[32] In the final step of the suggested mechanism for dioxygen reduction (see Figure 2), two protons and one electron are transferred to the Cu(II)-superoxide species formed in the previous step leading to the formation of H_2O_2. It has been suggested that protons from the C-2 and C-4 oxygens of TPQ_{sq} are involved in this process.[20] The first electron transfer from TPQ_{red} to dioxygen causes a large alteration in the pK_a value of TPQ_{sq},[29] facilitating a fast proton transfer from the C-2 oxygen of TPQ_{sq} to the Cu hydroxide species formed during the reductive half-reaction. The water molecule formed in this process is suggested to undergo a fast exchange by the superoxide anion.[20] Tyr305 is proposed to be a part of the hydrogen-bonded chain involved in the proton transfer from the C-4 oxygen of TPQ_{sq}.[20] Mutation of Tyr305 with alanine does not alter the rate of the reaction, indicating that a water molecule can take the role of Tyr305 in the hydrogen-bonded network.[35] The above detailed experimental information about the different steps combined with known X-ray structures provides a very good starting point for the present quantum chemical study of the mechanism. In the present study, apart from providing information regarding short-lived intermediates and transition states, the phenomenon of "spin catalysis" has been investigated. As discussed below, this enzyme is a perfect example for studying the spin transitions involving dioxygen because this step is likely to be rate-limiting.

II. Computational Details

All calculations discussed here were performed using the Gaussian 98[36] and Jaguar[37] programs. The transition states for all of the steps and the Hessians for all of the structures were calculated using the Gaussian 98 program. The rest of the calculations, including the optimization of all of the reactants and products, were performed using the Jaguar program. The calculations of the mechanism were performed in two steps. First, an optimization of the geometry was made using the B3LYP method[38] with the double-ζ quality *lacvp* basis set, which has an ECP[39] for the copper atom. The only exception is the first step, where in order to calculate the dioxygen binding, the *lacvp** basis set with a polarization function was used for dioxygen. Open-shell systems were treated using unrestricted B3LYP (UB3LYP). To stay reasonably close to the experimental structure, one atom of each histidine residue was kept frozen from the X-ray structure during the optimization. In the figures, frozen atoms are shown in rectangular boxes. All other degrees of freedom were optimized, and the transition states obtained were confirmed to have only one imaginary frequency of the Hessian. In the second step, the standard *lacv3p*** basis set of triple-ζ quality was used. This basis set includes one polarization function on each atom and an extended ECP on the copper atom. Zero-point vibrational and thermal enthalpy effects were added based on B3LYP calculations using the same basis set as was used for the geometry optimization. Since some atoms were kept frozen, reliable entropy effects could not be obtained; therefore, these effects were neglected. This is probably a reasonable approximation, even in the first step where dioxygen becomes bound, since this binding occurs at the same time a water molecule is released. The dielectric effects from the surrounding environment were obtained using the self-consistent reaction-field method as implemented in the Jaguar program.[40,41] A probe radius of $R = 1.40$ Å, corresponding to the water molecule, was chosen. The dielectric constant was set to 4, which corresponds to a dielectric constant of about 3 for the protein and 80 for the water medium surrounding the protein.[42] The relative energies discussed below include all of the effects described above. To test the accuracy of the B3LYP method for the present system, single-point calculations for all of the structures and full optimizations of only the reactants and products have been performed using only 15% of the exact exchange rather than 20% (B3LYP*).[43] These calculations reproduce the spin states obtained from the B3LYP optimizations and provide very similar energetics. The single-point calculations with B3LYP* quite consistently reduce the barriers only by 1.5−2.0 kcal/mol and increase the exothermicities marginally by 0.5−1.0 kcal/mol. The full optimization using B3LYP* has a slightly larger effect; it increases exothermicities for all of the steps by 2−3 kcal/mol. A comparison between the spin densities obtained from B3LYP and B3LYP* confirmed that the B3LYP method provides the correct spin states for the structures used in the present study. A few single-point calculations have also been attempted using the MP2 method to check for possible errors made by the B3LYP method in the treatment of charge-separated states. All of these attempts failed due to the large size of the models used in this study. Normal

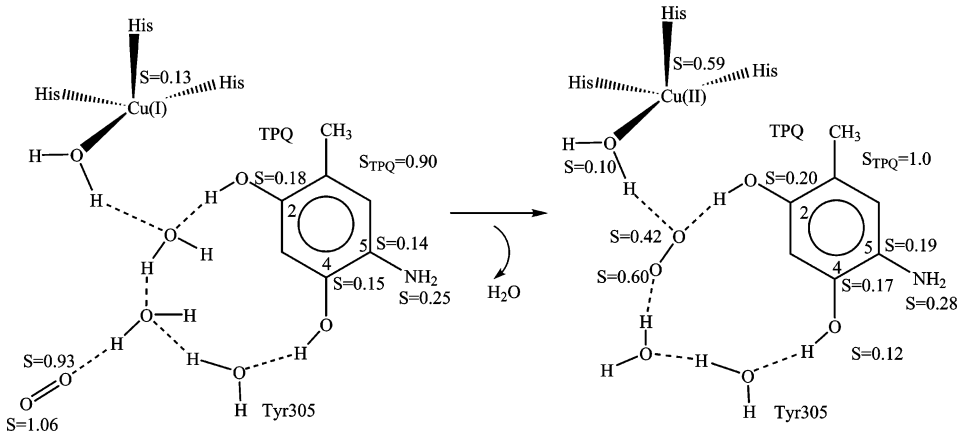

Figure 3. First step of the mechanism.

errors that occur by using B3LYP and different aspects of modeling enzyme active sites are described in recent reviews.[44−47]

III. Results and Discussion

The present quantum chemical study of H_2O_2 formation in the oxidative half-reaction of HPAO has been carried out using methods and models that are similar to those used in the reductive and oxidative half-reactions and the biogenesis of TPQ in CAOs.[25−27,48] An important question to be considered concerns the choice of a suitable model for the active site. Since the Cu-metal center is experimentally suggested to be extremely critical for H_2O_2 formation,[29,30] it was included in the model. To investigate the effect of Cu(II) on the mechanism, some of the steps were studied by substituting Cu(II) with Zn(II). The total charge of the system was chosen to be +2 and the reactant spin state as a quartet. The triplet oxygen and the Cu(II) ion can also be coupled to a doublet reactant state (eq A2), but at the initial steps of the reaction, where the superoxide ion (being coordinated to Cu) undergoes hydrogen abstraction from TPQ, the quartet and doublet (eq A2, see the Appendix) states behave in a similar manner. Thus, we use the quartet state to simulate the corresponding doublet, presented by eq A2. As discussed below, the system will later cross over to the second doublet potential energy surface. A neutral, reduced form of cofactor TPQ has been chosen here, as suggested experimentally.[29] Histidines are modeled by imidazoles, and on the basis of earlier experience for proton-transfer reactions, tyrosine is modeled as a water molecule. The overall reaction for dioxygen reduction to hydrogen peroxide can be written as

$$O_2 + TPQ_{aminoquinol} \rightarrow H_2O_2 + TPQ_{iminoquinone} \qquad (6)$$

Reaction 6 is calculated to be slightly endothermic by 2.1 kcal/mol, including dielectric effects. This result does not include the breakage and formation of hydrogen bonds in this process.

A. Step 1: Dioxygen Binding and Formation of a Superoxide Anion. In the first step of the suggested mechanism (see Figure 3), dioxygen replaces the axial water (W_a) and binds between the O-2 and O-4 positions of cofactor TPQ, as shown by the X-ray structure.[28] It has been assumed in the model that dioxygen has already left its earlier binding site, in the regions of Leu425, Met634, and Tyr407,[13] and is now positioned in the vicinity of the hydrogen-bonded network, connecting the O-2 and O-4 positions of the cofactor. In the first step, all of the relevant species, the copper complex, the reduced TPQ, Tyr305, O_2, and a water molecule, are involved. In the reactant, dioxygen is in a triplet state and very weakly bound to one of the water molecules in a hydrogen-bonded network. In this step, triplet dioxygen replaces the axial water molecule concomitantly with an electron transfer from TPQ_{red} to dioxygen. It has been observed experimentally in the wild-type- and Co-substituted HPAOs that after the first electron transfer, the displacement of a metal-bound water molecule takes place.[30] This electron transfer leads to the creation of a Cu(II)···O_2(rad)···M(rad) complex, where M(rad) represents the reduced semiquinol form of TPQ. On the basis of the experimentally measured O-18 kinetic isotope effects, the first electron transfer from TPQ_{red} to dioxygen has been suggested as rate-limiting for BSAO[29] and HPAO.[30] In the present DFT study, it was not possible to localize the transition state for the first electron transfer. Since this electron transfer is accompanied by the displacement of a metal-bound water molecule by dioxygen, the modeling of the transition state is extremely difficult. In the model calculations, a few attempts were made to calculate the reactant with triplet O_2 in the presence of TPQ, but all of these attempts failed. Whenever O_2 comes close to the reduced TPQ, an electron transfer from cofactor TPQ to O_2 takes place. Only after the addition of the extra polarization function on dioxygen could the reactant in this step be optimized. This step is calculated to be endothermic by 9.5 kcal/mol. The endothermicity of this step agrees well with experiments, which suggests that the formation of the superoxide anion is energetically unfavorable.[29] Surprisingly, the main part of this endothermicity comes from dielectric effects of 14.9 kcal/mol. Normally, one would expect dielectric effects (outer-sphere reorganization effects) to go in the other direction and stabilize the product of the electron transfer since the dipole moment of the product is normally larger. However, in this case, the reactant actually has a larger dielectric energy contribution since almost all of the +2 charge is localized on the copper-metal center. After the electron transfer from TPQ to dioxygen, TPQ and the Cu-superoxide moiety will have a +1 charge. Since the dielectric contribution depends on the square of the charge, this will lead to a contribution proportional to $2^2 = 4$ for the reactant but only $1^2 + 1^2 = 2$ for the product. No transition state for this step could be located, but it should be noted that an activation barrier of 6−8 kcal/mol could, in principle, make it rate-determining for the entire oxidative half-reaction, as suggested experimentally.[29,30]

B. Step 2: Interaction between Cu(II) and the Superoxide Anion. In the second step of the suggested mechanism (see Figure 4), the superoxide anion formed in the previous step moves and binds to Cu(II). An interaction between the superoxide anion and Cu(II) has been suggested by a mechanistic study in HPAO.[32] This interaction is also supported by the X-ray structure from ECAO,[28] where peroxide has been found to interact directly with Cu(II). This step has a barrier of 3.6 kcal/

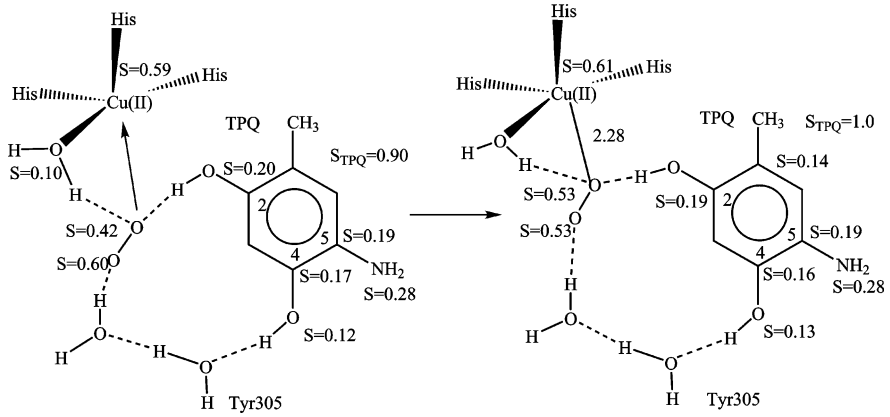

Figure 4. Second step of the mechanism.

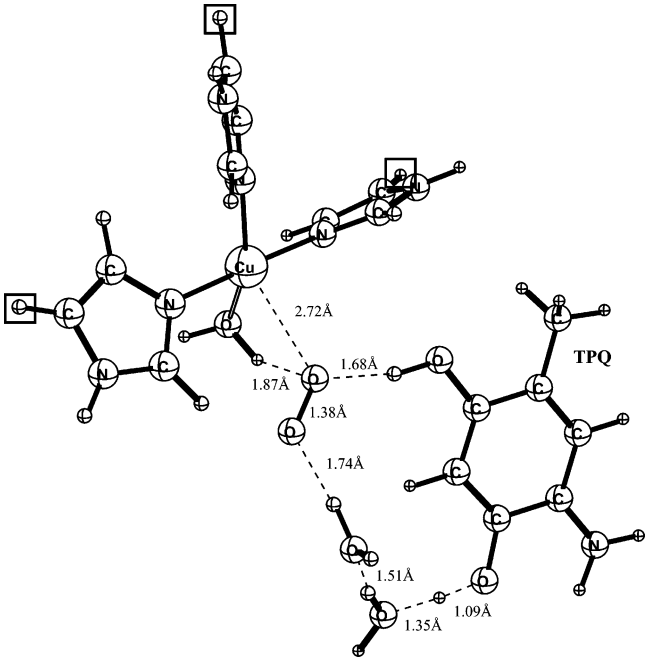

Figure 5. Optimized transition state for step 2.

mol, including solvent effects of >0.4 kcal/mol and zero-point vibrational (plus thermal enthalpy) effects of <0.3 kcal/mol. The optimized transition state for this step is shown in Figure 5. This step is slightly exothermic by 1.7 kcal/mol.

C. Step 3: Formation of Hydrogen Peroxide. In the final step of the suggested mechanism, the Cu(II)−superoxide species formed in the previous step should accept one electron and two protons from TPQ_{sq} to form hydrogen peroxide. In the crystal structure of ECAO, the product peroxide is in proximity of Cu(II).[28] Experimentally, an electron from TPQ_{sq} and protons from the C-2 and C-4 oxygens are suggested to participate in the H_2O_2 formation.[20] Proton transfer from the C-4 oxygen is experimentally proposed to occur through a hydrogen-bonded chain containing Tyr305 and a water molecule.[20,35] As mentioned above, reaction 6 is a spin-forbidden process. $TPQ_{aminoquinol}$, H_2O_2, and $TPQ_{iminoquinone}$ are all singlets. Cu(II) is a doublet, and O_2 is a triplet. For hydrogen peroxide production, a spin transition in the system is necessary somewhere along the reaction sequence. In principle, the necessary spin transition could occur when the superoxide binds to the metal center. However, the B3LYP calculations show that the doublet and quartet states are degenerate for the metal−dioxygen complex, which means that there is no exchange interaction among the three spins at this stage. Thus, there is no matrix element for the spin transition in the radical-pair $O_2^-\cdots$MH system (see the Appendix). The reason for this is that there is no covalent bonding between the superoxide and Cu(II) atoms, which would split the doublet and quartet states. Covalent binding would require the participation of Cu(III), but this state is apparently too high in energy to significantly participate in the bonding. In fact, in the Zn-substituted enzyme, the superoxide was calculated to form a significantly shorter bond with the metal. In the wild-type enzyme, the Cu−O bond distance is 2.30 Å, whereas in the Zn-substituted enzyme, the Zn−O bond distance is 2.10 Å. Therefore, it is concluded here that the spin transition does not occur until the final step of the dioxygen reduction to hydrogen peroxide.

Since there cannot be any spin crossing for the Cu(II)−superoxide radical pair, the system has to continue on the quartet surface. In the first part of this step (see Figure 6), one electron and two protons from the C-2 and C-4 positions of TPQ_{sq} are transferred in a concerted manner to the Cu(II)−superoxide species. This part has a very high barrier of 23.3 kcal/mol, including zero-point vibrational (plus thermal enthalpy) effects of <4.0 kcal/mol and solvent effects of >1.8 kcal/mol. The concerted $2H^+ + e^-$ transfer transition state is shown in Figure 7. A spin population of 0.5 on dioxygen and 1.5 on TPQ_{sq} and all of the relevant O−H bond distances indicate that this process is concerted. During this process, the spin on Cu(II) largely remains unchanged. This step leads to the formation of a high-energy, triplet excited state of cofactor TPQ (see Figure 8). The product is endothermic by 14.0 kcal/mol, including solvent effects of <4.1 kcal/mol. Since this step follows a step which is endothermic by 7.8 kcal/mol, the overall barrier for this step becomes very high (31.1 kcal/mol) and it is endothermic by 21.8 kcal/mol. After the formation of the triplet excited state of TPQ, the nonadiabatic quenching of this species produces hydrogen peroxide and singlet TPQ. From the creation of the Cu(II)−superoxide radical pair, the production of hydrogen peroxide is exothermic by 11.7 kcal/mol, where solvent effects contribute by <3.1 kcal/mol. Since the activation energy is very high, this reaction path on the quartet potential energy surface is ruled out.

From the above information, it is clear that the system has to undergo a spin transition before or during the proton- and electron-transfer step. Once the system is on the doublet surface, a concerted $2H^+ + e^-$ transfer from TPQ_{sq} can take place in exactly the same manner as on the quartet surface (see Figure 9). The optimized doublet transition state for this step is shown in Figure 10. The calculated imaginary frequency is 1348 cm^{-1}. In this case, the barrier is much lower (8.1 kcal/mol), including zero-point vibrational (plus thermal enthalpy) effects of <3.7

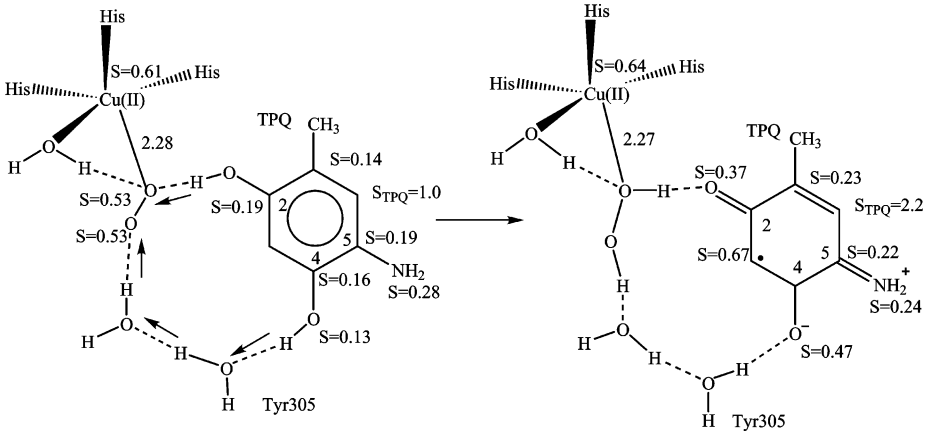

Figure 6. First part of step 3 of the mechanism on the quartet potential energy surface.

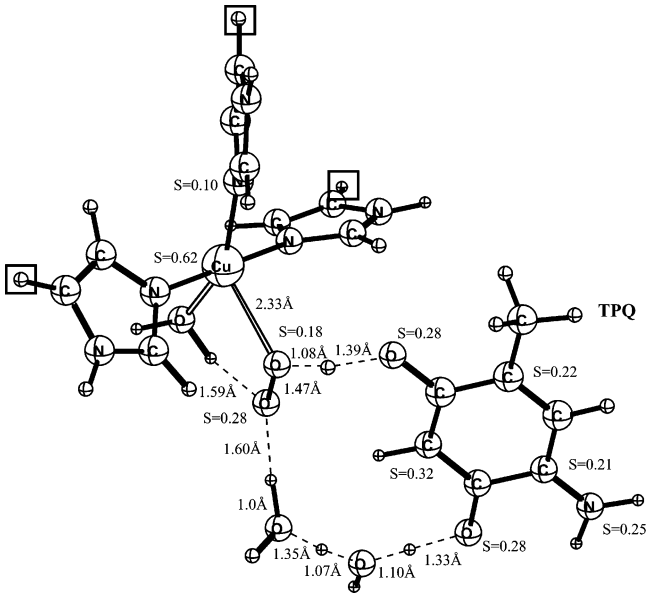

Figure 7. Optimized quartet transition state for step 3.

kcal/mol and solvent effects of 0.9 kcal/mol. In contrast to the mechanism on the quartet surface, this step directly leads to the creation of hydrogen peroxide.

To analyze the nature of the doublet transition state, shown in Figure 10, the molecular Hessian was used to calculate the isotope effects. Large deuterium isotope effects and almost no oxygen isotope effects were found. In contrast, experimentally no deuterium isotope effects and significant O-18 effects were measured.[29,30] Since the calculated isotope effects do not match the measured isotope effects, this transition state can therefore not be rate-limiting for the CAOs.

Partly on the basis of the above results, it is concluded here that instead of the first electron transfer, the spin transition in the third step is most likely the rate-limiting step. The spin crossing is suggested to be induced by the intermolecular vibrations between O_2^- and Cu(II), which involve the displacements of the oxygen atoms in dioxygen. A major additional reason for drawing the conclusion that a spin transition is rate-limiting is the experimental result that substitution of the paramagnetic Cu^{2+} with the diamagnetic Ni^{2+} and Zn^{2+} ions in HPAO resulted in substantially reduced catalytic activity, whereas substituting Cu^{2+} with paramagnetic Co^{2+} did not alter the enzyme activity.[32] Apparently, the presence of a metal spin is important. It is much more difficult to rationalize these findings if the first electron transfer is rate-limiting, as has been previously suggested.[29,30]

In the present study, the paramagnetic metal is suggested to accelerate the rate of the spin interconversion by spin catalysis of exchange type.[6,49] For enzymes containing metal ions, the driving force for the spin transition is an exchange interaction. The doublet in eq A2 of the Appendix represents the starting triplet state of the radical pair which correlates with the O_2 triplet, while the doublet state in eq A1 corresponds to the singlet state of the radical pair. Only the radical pair described by eq A1 can produce the final product. Thus, the reaction occurs on the doublet potential energy surface [in the presence of the Cu(II) ion] and includes the spin crossing between two doublet surfaces. The driving force for the spin recoupling is an exchange interaction which is explained in the Appendix. This suggestion is not in line with the generally accepted chemical rules for metal-coordinated complexes. The physical background for this peculiarity is connected with the spin catalysis concept.[49−52]

To address the issue of the spin crossing probability on the calculated potential energy surfaces, the formulas derived in the Appendix were used. The term k_2 (eq A8) is the main rate-limiting constant. According to the B3LYP calculations, the spin transition is most likely to occur somewhere between the transition states for the quartet and the doublet potential energy surfaces. By a pointwise search, an approximate crossing point between the different spin surfaces was located (see Figure 11). For this structure, all of the vibrational frequencies and their normal modes were calculated. The main promoting $Cu-O_2$ vibration is identified to be one with a frequency of $\omega = 106$ cm^{-1}. The energy splitting between the quartet and doublet states along this vibration was then calculated. It was estimated that

$$|\partial\langle\Psi_{1d}|V_S|\Psi_{2d}\rangle/\partial Q_p|^2 = 29.16\ (\text{kcal/mol})^2\ \text{Å}^{-2}$$

The derivative is thus equal to 5.4 (kcal/mol) $Å^{-1}$, which is suggested to be the vibronic perturbation which promotes the spin transition in the system. This vibronic matrix element is higher than the corresponding vibronic matrix elements that are responsible for the Jahn−Teller (and pseudo-Jahn−Teller) effects in a number of Cu-containing complexes (including tunneling, vibronic reduction of spin−orbit coupling splitting, **g**-tensor in ESR spectra, and IR and electronic spectra).[53,54] Similar vibronic matrix elements have also been obtained for CuF_6^{4-}, $Cu(H_2O)_6^{2+}$, and $CuCl_4$ complexes.[55−58] The estimated rate constant for the spin−flip step itself is therefore quite large, $k_2 = 8 \times 10^{10}\ s^{-1}$ (see the Appendix).

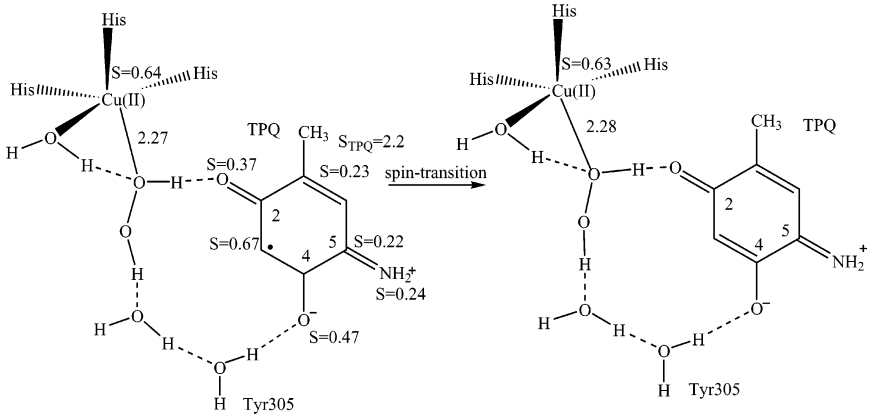

Figure 8. Second part of step 3 of the mechanism on the quartet potential energy surface.

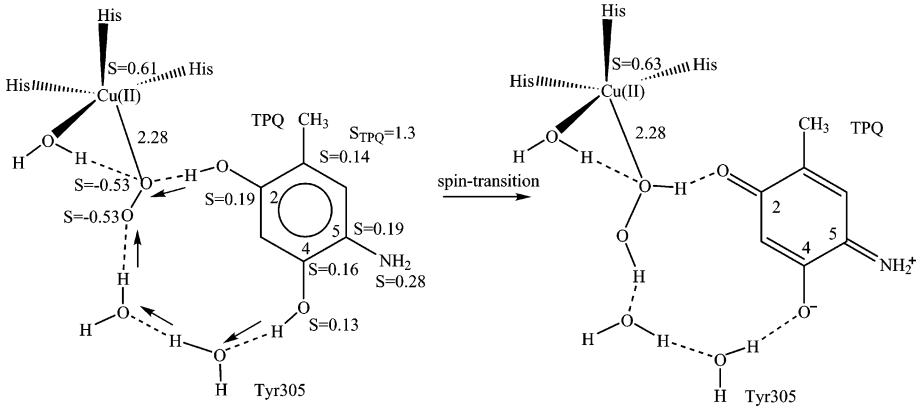

Figure 9. Step 3 of the mechanism on the doublet potential surface.

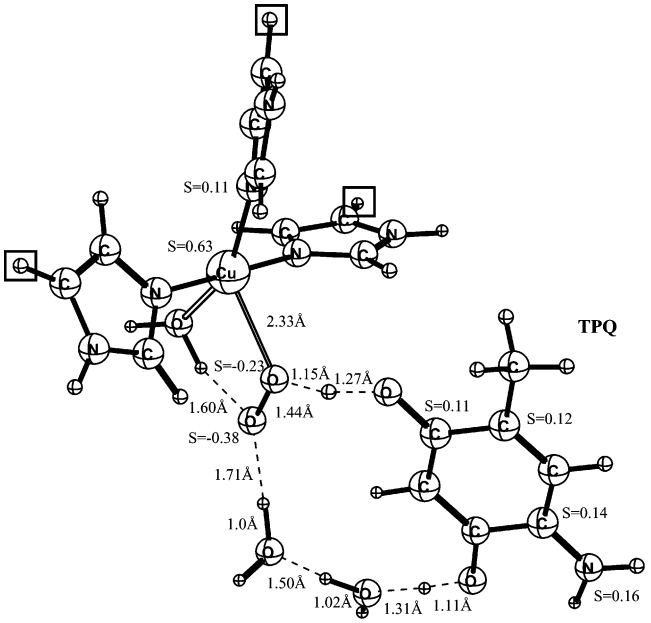

Figure 10. Optimized doublet transition state for step 3.

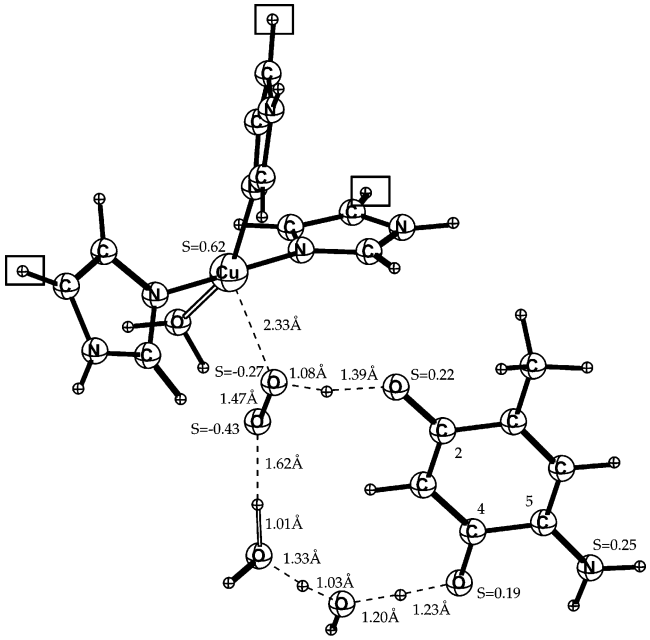

Figure 11. Crossing point between the quartet and doublet potential surfaces.

The dipole transition integral in the harmonic approximation is equal to

$$|\langle 0|Q_p|1\rangle|^2 = \frac{\hbar}{2m_p\omega_p}$$

where m_p is the reduced mass of the Q_p vibration.

The spin crossing (in the region of the structure in Figure 11) is estimated to be approximately 10−12 kcal/mol greater than the reactant of this step. From the resting state of the enzyme, the overall barrier for the spin transition is 18−20 kcal/mol. The estimated barrier for this transition is in reasonable agreement with the experimentally measured barrier of 15.8 kcal/mol for the rate-limiting step.[32]

The measured O-18 isotope effect can also be rationalized by this type of rate-limiting spin transition. The difference in the O−O bond distance between the spin-crossing point and the resting state before dioxygen becomes bound is then the

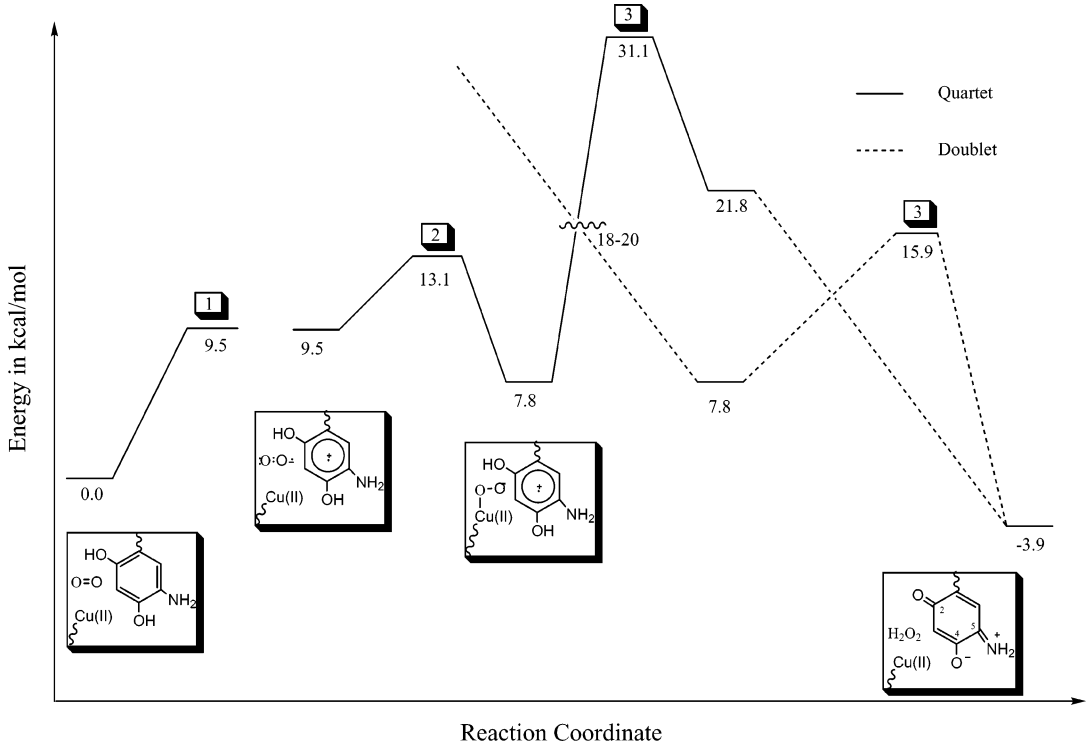

Figure 12. Energy diagram for the dioxygen reduction in the oxidative half-reaction of CAO.

likely origin of the shift. Actually calculating an accurate isotope shift proved to be too difficult. The primary reason behind this problem is that the oxygen isotope effect is very small (ca. 1%).

As noted above, no catalysis is observed for the Zn-substituted enzyme. According to the present calculations for the Zn-containing enzyme, it should follow almost exactly the same energetics as the wild-type Cu enzyme. The X-ray structure of the Ni-substituted AGAO is much more similar to the native enzyme than the Zn-substituted one. Therefore, the Ni-substituted HPAO is also expected to follow the same energetics as the native and Zn-substituted enzymes. The only difference is that in the absence of an unpaired spin on Zn and Ni, spin catalysis is not possible and the intersystem crossing cannot occur.

IV. Summary

In the present study, computational methods and models similar to those used for studying the biogenesis of TPQ,[48] the reductive half-reaction,[25,26] and the oxidative half-reaction[27] have been used. The present study was strongly guided by the large amount of structural and spectroscopic information provided by those experiments. As shown in Figure 12, the energy diagram for the mechanism suggested in the present study can be divided into three steps. The last step was studied for two different (quartet and doublet) potential energy surfaces. The energy diagrams are constructed by imposing the condition that the reactant of each step has the same energy as the product of the previous step. The mechanism for the formation of hydrogen peroxide in the oxidative half-reaction of CAOs can be summarized as follows. At the starting point of the suggested mechanism, dioxygen is weakly bound in the active-site cavity. As suggested experimentally,[29] it replaces the axial water molecule that is coordinated to Cu and occupies a cavity between the O-2 and O-4 positions of the TPQ cofactor. Dioxygen binding takes place with a simultaneous electron transfer from TPQ_{red} to dioxygen, which results in the formation of a Cu(II)···O_2(rad)···M(rad) complex, where M(rad) represents the semiquinol form of TPQ. Dioxygen binding is calculated to be endothermic by 9.5 kcal/mol. The endothermicity of this step is in line with experimental results.[29] In the model calculations, an activation barrier for this electron transfer could not be calculated. However, a barrier of 6−8 kcal/mol for this electron transfer could, in principle, make this the rate-limiting step in the oxidative half-reaction. In the second step, the superoxide anion formed in the previous step moves over and binds to Cu(II), as suggested experimentally.[28,32] This step has a barrier of 3.6 kcal/mol and is slightly exothermic by 1.7 kcal/mol. From the resting state of the enzyme, the overall barrier for this step is 13.1 kcal/mol, and it is 7.8 kcal/mol endothermic.

Since the formation of H_2O_2 is a spin-forbidden process, the system has to undergo a spin transition. In the presence of the paramagnetic Cu(II) ion, this spin transition corresponds to the nonadiabatic doublet−doublet transition between the PES of the Ψ_{1r} and Ψ_{2r} states (eqs A1 and A2). In the absence of any covalent bonding between the metal and the superoxide ion, the electron−electron interaction induces a weak exchange interaction between the spin of the metal and the two spins in the radical pair. This weak exchange interaction is responsible for the spin transition in the system. However, for the weakly bound Cu−O_2 complex, no spin transition can take place because the doublet and quartet states are degenerate at this point. The degeneracy of these states means that there is no exchange interaction between the three spins and, hence, no matrix element for the spin transition.

Instead, the system that is formed can either follow the quartet surface or cross over to the doublet surface. On the quartet surface, there is a very high barrier of 31.1 kcal/mol and a highly endothermic triplet excited-state TPQ is formed. Eventually through nonadiabatic quenching, hydrogen peroxide and singlet TPQ can be produced. However, the barrier for this step is too high, and a reaction on the quartet potential energy surface is therefore ruled out.

The only option left is to make a spin crossover to the doublet surface in the final step. On the doublet surface, a concerted

$2H^+ + e^-$ transfer from TPQ_{sq} similar to that of the quartet state can take place but with a much lower barrier of 8.1 kcal/mol, which directly leads to the formation of hydrogen peroxide. Calculating the Hessian for this transition state, we found large deuterium isotope effects but no O-18 isotope effects, which contradicts the experimental isotope effects.[29,30] These results therefore indicate that passing this transition state is not rate-limiting in the catalytic cycle. On the basis of the experimental results regarding the role of the Cu-metal center, it is here suggested that the step involving the spin transition is the rate-limiting step. This transition should be triggered by the calculated vibronic perturbation of 5.4 (kcal/mol) $Å^{-1}$ at the crossing point between the potential surfaces. This value for the coupling leads to a very fast rate of 8×10^{10} s^{-1} for the spin transition itself, but since the transition occurs at such a high energy, this step would still be rate-limiting. The origin of the experimentally measured O-18 isotope effect is suggested to be the difference in the O−O bond distances between the resting state (free dioxygen) and this state. Pointwise calculations indicate that the spin transition should occur near the transition state on the doublet surface. The estimated barrier is 18−20 kcal/mol from the resting state of the enzyme, which is in reasonable agreement with the experimentally measured barrier of 15.8 kcal/mol for the rate-limiting step.[32] When spin catalysis is included in the rate-limiting step, the quite puzzling effects noted experimentally when copper is substituted by other metals are readily explained. Since spin on the metal is required, substitution by Ni and Zn should destroy the catalytic activity, while substitution with Co should preserve it, which agrees with the experimental observations. It would be much more difficult to rationalize these findings if the electron transfer in the first step would be rate-limiting, as has been suggested.[29,30] However, it has to be mentioned that the mechanism suggested in the present study is not used by all known CAOs. CAOs from different species have been suggested to have significant differences; for example, the Ni(II)-substituted bacterial AGAOs have been observed to exhibit some amount of catalytic activity.[15] The issue of spin transitions is quite important for dioxygen activation by enzymes. Whenever dioxygen is involved, this issue has to be addressed. It is suggested that many other enzymes (other than the CAOs) use a paramagnetic metal to overcome the spin prohibition.

V. Appendix

Intersystem Crossing (ISC). There are three radicals in the $MH^+\cdots O_2^-\cdots$Cu(II) system, denoted as b···x···d, where each radical has one unpaired electron. The wave function of the ground state of this three-electron system is represented by the doublet-state wave function

$$\Psi_{1r} = 2^{-1/2}(|b\bar{x}d| + |x\bar{b}d|) \tag{A1}$$

This diabatic state represents the ground state of the reactants with singlet spin pairing in the RP $MH^+\cdots O_2^-$, $^1\Psi_{x,b}$. The paramagnetic metal ion is represented by one d electron. The corresponding triplet RP state can be written as the doublet state

$$\Psi_{2r} = 6^{-1/2}(|b\bar{x}d| - |x\bar{b}d| + 2|b\bar{d}x|) \tag{A2}$$

and as the quartet state

$$\Psi_q = |bxd| \tag{A3}$$

In the calculations, the Ψ_{2r} state has been simulated by the quartet state, Ψ_q (eq A3), since these states should behave in a similar manner and are inactive inside the RP moiety. They are degenerate in the beginning and are also expected to be quasi-degenerate along the superoxide binding reaction path. The Ψ_{2r} and Ψ_q states cannot correlate with the final diamagnetic product of H_2O_2. The energies of the two doublet structures (eqs A1 and A2) are equal to

$$E_{1,2} = Q \pm \sqrt{\frac{1}{2}[(J_{1,2} - J_{1,3})^2 + (J_{1,2} - J_{2,3})^2 + (J_{1,3} - J_{2,3})^2]} \tag{A4}$$

where the $J_{i,j}$ values are the exchange integrals, and Q is predominantly the Coulomb term.[59] The expression (eq A4) corresponds to the well-known London's formula. The indices 1, 2, and 3 denote the π_x, b, and d orbitals, where b is the singly occupied orbital of the TPQ cation radical, d is the singly occupied 3d orbital of the Cu(II) ion, and π_x and π_y are the π_g MOs of molecular oxygen. The exchange integral $J_{1,2}$ determines the singlet−triplet (S−T) splitting of the RP $O_2^-\cdots MH^+$, which according to the DFT calculations of the S and T states of the RP, is almost negligible. The integral $J_{2,3}$ is much larger than $J_{1,3}$ since the third spin is further from the Cu ion, and is it localized on the TPQ cofactor. The quartet-state energy is equal to $Q + (J_{1,2} + J_{1,3} + J_{2,3})$, and this state is nonreactive like the starting triplet state of the RP. The copper ion works as a spin catalyst and promotes the nonradiative transition between the two doublet states (eqs A1 and A2), which are actually the singlet and triplet states of the $O_2^-\cdots MH^+$ radical pair. The system starts in the triplet RP state (eq A2). Then, weak intermolecular vibrations between O_2^- and Cu(II) produce a modulation of the $J_{2,3}$ exchange integral (integral $J_{1,3}$ is very small). Since the spin exchange in the system is strongly nonsymmetric ($J_{2,3} \gg J_{1,3}$), the α- and β-spins in the 2−3 pair exchange must faster than in the 1−3 pair. An account of the spin evolution in such a system indicates that the spin transition occurs in the 1−2 radical pair.[52,60,61] The rate constant of the ISC is proportional to $(J_{2,3} - J_{1,3})^2$.[52] This exchange interaction is the driving force for this type of spin catalysis. It can be illustrated by the following simple scheme:

$$MH^+(\uparrow) + O_2^-(\uparrow) + \text{Cu(II)}(\downarrow) \rightarrow MH^+(\uparrow) + O_2^-(\downarrow) + \text{Cu(II)}(\uparrow) \tag{A5}$$

The rate of exchange in the $O_2^-\cdots$Cu(II) pair is much faster than it is in the other pairs. The total spin of the whole enzyme is not changed (i.e., all states are doublets). The exchange interaction of $O_2^-\cdots$Cu(II) can include a superexchange through the ligand (OH group).[60] The rate constant for the nonradiative, nonadiabatic transition between the two doublet potential energy surfaces (PES), which corresponds to the triplet−singlet transition inside the $MH^+\cdots O_2^-$ ion radical pair, is given by Fermi's golden rule[62]

$$k = \frac{2\pi\rho}{\hbar}|\langle\Psi_{1d}|V|\Psi_{2d}\rangle|^2 \mathrm{FC} \tag{A6}$$

where ρ is the density of final states, FC is the Franck−Condon factor, and V is the perturbation operator; it is chosen here as a sum of an exchange interaction V_S and a non-Born−Oppenheimer (NBO) term:

$$V = V_S + V_{NBO}$$

where

$$V_{NBO} = H_0 - H_{BO} = \sum_p \frac{\partial}{\partial Q_p} Q_p$$

and

$$V_S = \sum_{i,j} J_{i,j} S_i S_j$$

Here, Q_p is the vibrational mode. Wave functions are considered as depending not only on electronic variables (r) but also on nuclear displacements (Q) from the equilibrium, $^2\Psi_1(r, Q)$. The breakdown of the Born−Oppenheimer approximation is responsible for the mixing of the vibrational and the electronic wave functions.

Equation A6 can be written as

$$k = k_1 + k_2$$

where

$$k_1 = \frac{2\pi\rho}{\hbar} |\langle \Psi_{1d} | V_S | \Psi_{2d} \rangle|^2 \mathrm{FC} \qquad \text{(A7)}$$

$$k_2 = \frac{2\pi\rho}{\hbar} \sum_p |\partial \langle \Psi_{1d} | V_S | \Psi_{2d} \rangle / \partial Q_p|^2 \mathrm{FC}\ |\langle 0 | Q_p | 1 \rangle|^2 \qquad \text{(A8)}$$

In eq A8, the Franck−Condon factor (FC) includes in each summation step all modes except Q_p, and the integral

$$|\langle 0 | Q_p | 1 \rangle|^2 \qquad \text{(A9)}$$

considers the ground-state vibrational level and the first excited vibrational level of the Q_p mode. The first term is calculated at the fixed geometry of the quartet−doublet crossing point, and the second term includes the dependence of exchange interaction on the nuclear displacements along the reaction coordinate. Q_p can be the normal modes which are perpendicular to the reaction coordinate (internal vibrations inside the reactants). These contributions are supposed to be negligible. Among the Q_p modes, the reaction coordinate Q_r can be considered as a special contribution.

The global FC factor can be estimated to be 10^{-6} as a lower limit. The density of states is estimated by the typical vibrational relaxation time in a solvent: $\tau = \rho\hbar = 10^{-11}$ s. The integral (eq A9) is equal to 0.01 Å^2. Finally, the spin−flip rate constant is estimated as $k_2 = 7.8 \times 10^{10}$ s^{-1}.

References and Notes

(1) Klinman, J. P. *J. Biol. Inorg. Chem.* **2001**, *6*, 1.
(2) Sawyer, D. T. *Oxygen Chemistry*; Oxford University Press: New York, 1991.
(3) Minaev, B. *Russ. J. Struct. Chem.* **1982**, *23*, 170.
(4) Minaev, B. *Sov. J. Chem. Phys.* **1985**, *3*, 1533.
(5) Prabhakar, R.; Minaev, B. F.; Siegbahn, P. E. M. *Biochim. Biophys. Acta* **2002**, *1647*, 173−178.
(6) Prabhakar, R.; Siegbahn, P. E. M.; Minaev, B. F.; Ågren, H. *J. Phys. Chem. B* **2002**, *106*, 3742−3750.
(7) Eastman, M.; Kooser, R.; Das, M.; Freed, J. *J. Chem. Phys.* **1969**, *51*, 2690.
(8) Kivelson, D. *J. Chem. Phys.* **1960**, *33*, 1094.
(9) Freed, J. *J. Phys. Chem.* **1967**, *71*, 38.
(10) Davidson, V. L. *Principles and application of Quinoproteins*; Marcel Dekker, Inc.: New York, 1993; pp 3−14.
(11) Parsons, M. R.; Convery, M. A.; Wilmot, C. M.; Yadav, K. D. S.; Blakeley, V.; Corner, A. S.; Phillips, S. E. V.; McPherson, M. J.; Knowles, P. F. *Structure* **1995**, *3*, 1171−1184.
(12) Kumar, V.; Dooley, D. M.; Freeman, C. H.; Guss, J. M.; Harvy, I.; McGuirl, M. A.; Wilce, M. C. J.; Zubak, V. M. *Structure* **1996**, *4*, 943−955.
(13) Li, R.; Klinman, J. P.; Mathews, F. S. *Structure* **1998**, *6*, 293−307.
(14) Wilce, M. C. J.; Dooley, D. M.; Freeman, C. H.; Guss, J. M.; Matsunami, H.; McIntire, W. S.; Ruggiero, C. E.; Tanizawa, K.; Yamaguchi, H. *Biochemistry* **1997**, *36*, 16116−16133.
(15) Kishishita, S.; Okajima, T.; Kim, M.; Yamaguchi, H.; Hirota, S.; Suzuki, S.; Kuroda, S.; Tanizawa, K.; Mure, M. *J. Am. Chem. Soc.* **2003**, *125*, 1041−1055.
(16) Klinman, J. P. *J. Biol. Chem.* **1996**, *271*, 27189−27192.
(17) Dooley, D. M. *J. Biol. Inorg. Chem.* **1999**, *4*, 1−11.
(18) Klinman, J. P. *Chem. Rev.* **1996**, *96*, 2541−2561.
(19) Stubbe, J.; Van der donk, W. A. *Chem. Rev.* **1998**, *98*, 705−762.
(20) Mure, M.; Mills, S. A.; Klinman, J. P. *Biochemistry* **2002**, *41*, 9269−9278.
(21) Hartmann, C.; Brzovic, P.; Klinman, J. P. *Biochemistry* **1993**, *32*, 2234−2241.
(22) Cai, D.; Dove, J.; Nakamura, N.; Sanders-Loehr, J.; Klinman, J. P. *Biochemistry* **1997**, *36*, 11472−11478.
(23) Hevel, J. M.; Mills, S. A.; Klinman, J. P. *Biochemistry* **1999**, *38*, 3683−3693.
(24) Dooley, D. M.; McGuirl, M. A.; Brown, D. E.; Turowski, P. N.; McIntire, W. S.; Knowles, P. F. *Nature* **1991**, *349*, 262−264.
(25) Prabhakar, R.; Siegbahn, P. E. M. *J. Phys. Chem. B* **2001**, *105*, 4400−4408.
(26) Prabhakar, R.; Siegbahn, P. E. M. *J. Comput. Chem.* **2003**, *24*, 1599−1609.
(27) Prabhakar, R.; Siegbahn, P. E. M. *J. Phys. Chem. B* **2003**, *107*, 3944−3953.
(28) Wilmot, C. M.; Hajdu, J.; McPherson, M. J.; Knowles, P. F.; Phillips, S. E. V. *Science* **1999**, *286*, 1724−1728.
(29) Qiaojuan, S.; Klinman, J. P. *Biochemistry* **1998**, *37*, 12513−12525.
(30) Mills, S. A.; Goto, Y.; Su, Q.; Plastino, J.; Klinman, J. P. *Biochemistry* **2002**, *41*, 10577−10584.
(31) Mure, M.; Klinman, J. P. *J. Am. Chem. Soc.* **1993**, *115*, 7117−7127.
(32) Mills, S. A.; Klinman, J. P. *J. Am. Chem. Soc.* **2000**, *122*, 9897−9904.
(33) Drummond, J. T.; Matthews, R. G. *Biochemistry* **1994**, *33*, 3732−3741.
(34) Karlin, K. D.; Gultneh, Y. *Prog. Inorg. Chem.* **1998**, *35*, 219−327.
(35) Nakamura, N.; Moenne-Loccoz, P.; Tanizawa, K.; Mure, M.; Suzuki, S.; Klinman, J. P.; Sanders-Loehr, J. *Biochemistry* **1997**, *36*, 11479−11486.
(36) Frisch, M. J.; Trucks, G. W.; Schlegel, H. B.; Scuseria, G. E.; Robb, M. A.; Cheeseman, J. R.; Zakrzewski, V. G.; Montgomery, J. A., Jr.; Stratmann, R. E.; Burant, J. C.; Dapprich, S.; Millam, J. M.; Daniels, A. D.; Kudin, K. N.; Strain, M. C.; Farkas, O.; Tomasi, J.; Barone, V.; Cossi, M.; Cammi, R.; Mennucci, B.; Pomelli, C.; Adamo, C.; Clifford, S.; Ochterski, J.; Petersson, G. A.; Ayala, P. Y.; Cui, Q.; Morokuma, K.; Malick, D. K.; Rabuck, A. D.; Raghavachari, K.; Foresman, J. B.; Cioslowski, J.; Ortiz, J. V.; Stefanov, B. B.; Liu, G.; Liashenko, A.; Piskorz, P.; Komaromi, I.; Gomperts, R.; Martin, R. L.; Fox, D. J.; Keith, T.; Al-Laham, M. A.; Peng, C. Y.; Nanayakkara, A.; Gonzalez, C.; Challacombe, M.; Gill, P. M. W.; Johnson, B. G.; Chen, W.; Wong, M. W.; Andres, J. L.; Head-Gordon, M.; Replogle, E. S.; Pople, J. A. *Gaussian 98*, revision A.7; Gaussian, Inc.: Pittsburgh, PA, 1998.
(37) *JAGUAR 4.1*; Schrödinger, Inc.: Portland, Oregon, 2000. Vacek, G.; Perry, J. K.; Langlois, J.-M. *Chem. Phys. Lett.* **1999**, *310*, 189−194.
(38) Becke, A. D. *Phys. Rev. A* **1988**, *38*, 3098. Becke, A. D. *J. Chem. Phys.* **1993**, *98*, 1372. Becke, A. D. *J. Chem. Phys.* **1993**, *98*, 5648.
(39) Hay, P. J.; Wadt, W. R. *J. Chem. Phys.* **1985**, *82*, 299−310.
(40) Tannor, D. J.; Marten, B.; Murphy, R.; Friesner, R. A.; Sitkoff, D.; Nicholls, A.; Ringnalda, M.; Goddard, W. A., III; Honig, B. *J. Am. Chem. Soc.* **1994**, *116*, 11875−11882.
(41) Marten, B.; Kim, K.; Cortis, C.; Friesner, R. A.; Murphy, R. B.; Ringnalda, M.; Sitkoff, D.; Honig, B. *J. Phys. Chem.* **1996**, *100*, 11775−11788.
(42) Blomberg, M. R. A.; Siegbahn, P. E. M.; Babcock, G. T. *J. Am. Chem. Soc.* **1998**, *120*, 8812−8824.
(43) Reiher, M.; Salomon, O.; Hess, B. *Theor. Chem. Acc.* **2001**, *107*, 48−55.
(44) Siegbahn, P. E. M.; Blomberg, M. R. A. *Annu. Rev. Phys. Chem.* **1999**, *50*, 221−249.
(45) Siegbahn, P. E. M.; Blomberg, M. R. A. *Chem. Rev.* **2000**, *100*, 421−437.
(46) Blomberg, M. R. A.; Siegbahn, P. E. M. *J. Phys. Chem. B* **2001**, *105*, 9375−9386.
(47) Siegbahn, P. E. M. *Q. Rev. Biophys.* **2003**, *36*, 91−145.

(48) Prabhakar, R.; Siegbahn, P. E. M. *J. Am. Chem. Soc.* **2004**, *126*, 3996−4006.
(49) Minaev, B. F.; Ågren, H. *Czech. Chem. Commun.* **1995**, *60*, 339.
(50) Minaev, B. F.; Ågren, H. *Int. J. Quantum Chem.* **1996**, *57*, 510.
(51) Buchachenko, A.; Ruban, L.; Step, E.; Turro, N. *Chem. Phys. Lett.* **1995**, *233*, 315.
(52) Buchachenko, A.; Berdinsky, V. *Kinet. Catal.* **1996**, *37*, 615.
(53) Bersuker, I. B. *The Jahn−Teller effect and vibronic interactions in modern chemistry*; Plenum Press: New York, 1984; p 320.
(54) Englman, R. *The Jahn−Teller effect in molecules and crystals*; Wiley: London, 1972; p 350.
(55) Ballhausen, C. J.; Jahansen, H. *Mol. Phys.* **1966**, *10*, 183−184.
(56) Clack, D. W. *J. Chem. Soc. A* **1972**, 299−304.
(57) Ballhausen, C. J.; De Heer, J. *J. Chem. Phys.* **1965**, *43*, 4304.
(58) Moskowitz, J. W. *J. Chem. Phys.* **1970**, *53*, 2570−2580.
(59) Bonacic-Koutecky, V.; Koutecky, J.; Salem, L. *J. Am. Chem. Soc.* **1977**, *99*, 842.
(60) Minaev, B. F. *Theor. Exp. Chem.* **1996**, *32*, 1.
(61) Minaev, B. F. *Mol. Eng.* **1996**, *6*, 261.
(62) Metz, F.; Friedrich, S.; Hohlneicher, G. *Chem. Phys. Lett.* **1972**, *16*, 353.